Single Molecule Conductance of Porphyrin Wires with Ultralow Attenuation

ARTICLE *in* JOURNAL OF THE AMERICAN CHEMICAL SOCIETY · AUGUST 2008

Impact Factor: 12.11 · DOI: 10.1021/ja802281c · Source: PubMed

The experimental determination of the conductance of single molecules

Richard J. Nichols,*[a] Wolfgang Haiss,[a] Simon J. Higgins,[a] Edmund Leary,[ab] Santiago Martin[ac] and Donald Bethell[a]

Received 21st October 2009, Accepted 7th January 2010
First published as an Advance Article on the web 3rd February 2010
DOI: 10.1039/b922000c

The measurement of the electrical properties of molecules, down to the single molecule level, has become an experimental reality in recent years. A number of methods are now available for experimentally achieving this feat. The common aim of these methods is to entrap a single or small numbers of molecules between a pair of metallic contacts. This topical review focuses on describing and comparing experimental methods for entrapping and measuring the electrical properties of single molecules in metallic contact gaps. After describing the methods, reasons are tendered for apparent discrepancies in the literature between measured single molecule conductance values, with a focus on the most widely studied alkanedithiol system. Illustrative examples are then presented of the determination of the electrical properties of a range of single molecular systems, in order to highlight the progress which has been made in recent years.

1. Introduction

The measurement of the electrical properties of molecules, down to the single molecule level, has become an experimental reality in recent years. A number of methods are now available for experimentally achieving this feat. The common aim of these methods is to entrap a single or small numbers of molecules between a pair of metallic contacts as illustrated in Fig. 1.[1–8] The most commonly used methods for single molecule electrical property determination employ either an STM,[1,3,4] a conducting AFM,[2] or break junctions[6–11] to trap molecules between metal contacts. Importantly, these methods have enabled structure–property relationships to be explored in single molecule electronics and to address in a defined and systematic fashion the fascinating question of how electrical current flows through molecular junctions.[12] In particular

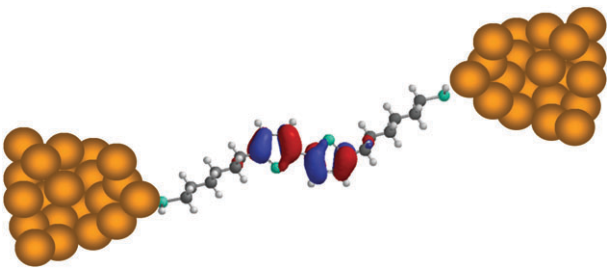

Fig. 1 Schematic illustration of a metal–molecule–metal junction.

[a] *Department of Chemistry, University of Liverpool, Crown Street, UK L69 7ZD. E-mail: nichols@liv.ac.uk; Tel: 0044 151 794 3533*
[b] *IMDEA Nanociencia, Departamento de Física de la MateriaCondensada, Modulo 13, Universidad Autónoma de Madrid, E-28049 Madrid, Spain*
[c] *Department of Organic and Physical Chemistry, University of Zaragoza, Campus Universitario, 50009 Zaragoza, Spain*

Richard J. Nichols

Richard J. Nichols is a Professor of Physical Chemistry at Liverpool University. He is an expert in the field of scanning probe microscopy, particularly as applied to in situ *electrochemical measurements. He has over 100 publications in peer-reviewed journals, many of which involve the application and development of probe microscopy techniques. His key area of research from 2001 has been in developing single molecule measurement techniques using the scanning tunnelling microscope (STM), in particular for the measurement of electrical properties. Professor Nichols is a Fellow of the International Society of Electrochemistry.*

Wolfgang Haiss

Wolfgang Haiss obtained his PhD from the Technical University Berlin in 1994. His research interests include molecular electronics, surface stress, electrochemistry and optical properties of small particles. He has over 40 publications in peer-reviewed journals and developed experimental methods for the measurement of single molecule conductance. He is a member of the German Physical Society and works currently as a post doctoral research fellow at the University of Liverpool.

this has facilitated detailed examination of the influence of chemical and electronic structure on the transmission of molecular electronic junctions. This has included the effect of conformation[13–16] and redox state[3,17–25] on single molecule conductance. Environmental influences on the electronic transmission of single molecule bridges have also been examined,[24,26,27] including the influence of solvent[24,26] for measurements under ambient conditions and the influence of temperature.[24,28–30]

This topical review focuses on describing and comparing experimental methods for entrapping and measuring the electrical properties of single molecules in metallic contact gaps. After describing the methods, reasons are tendered for apparent discrepancies in the literature between measured single molecule conductance values, with a focus on the most widely studied alkanedithiol system. Methods are discussed for obtaining important complementary information for the junctions, which includes the distance at which junctions cleave when stretched and the force required to cleave a metal–molecule–metal junction. Finally, we present a number of examples from the recent literature where structure–property relationships have been investigated using single molecule conductance determination.

2. The methods

2.1 Break junctions

Break junctions have provided a powerful platform for forming conducting nanowires and fabricating nanogap junctions with controllable separation, whose width can be adjusted to accommodate molecular bridges. There are several categories of break junctions, including those formed mechanically, those formed by electromigration, or junctions generated *in situ* using an STM; the latter is covered in the section 2.3. In 1985 Moreland and Ekin developed a method for mechanically forming tunnelling junctions by breaking thin and brittle Nb–Sn filaments mounted on a flexible glass beam.[31] Contact separation in these "break junctions" could be adjusted by varying the bending of the beam. In 1992 Muller *et al.* developed this method to form break junctions of non-brittle materials (*e.g.* metals) attached to a bending beam.[32] The term

Simon J. Higgins

Simon J. Higgins obtained his degree (1981) and PhD (1984) from the University of Southampton. After postdoctoral work at the Universities of Leeds (1984–7) and Oxford (1987–9), he was appointed to a Lectureship in Inorganic Chemistry at the University of Liverpool, where he is currently a Reader. His research interests are in organic and molecular electronics, and in structure–property relationships in single molecule electrical properties.

Edmund Leary

Edmund Leary obtained his PhD in Chemistry at the University of Liverpool (UK) in 2008. He is currently a postdoctoral researcher at the Instituto Madrileño de Estudios Avanzados (IMDEA) en nanociencia in Madrid, studying electronic transport through single molecules and nanoscale systems.

Santiago Martin

Santiago Martin received his PhD degree in physical chemistry in 2005 at the Zaragoza University (Spain) for studies on modified electrodes using the Langmuir–Blodgett technique. He held a Marie-Curie fellowship (2006–2007) and a post-doctoral fellowship (2007–2009) from the Spanish Government whilst working in Prof. R. J. Nichols' group. Presently he is a researcher within the "Juan de la Cierva" programme funded by the Spanish Government at Zaragoza University. His research interests include molecular electronics, electrochemistry, self-assembled chemistry, and thermodynamics. He is co-author of more than 30 publications in these areas.

Donald Bethell

Don Bethell is Emeritus Professor of Chemistry at the University of Liverpool. His special interest throughout his career has been Physical Organic Chemistry, with special emphasis on reaction kinetics and mechanism, catalytic phenomena, and more recently, functional nanostructures and molecular electronics.

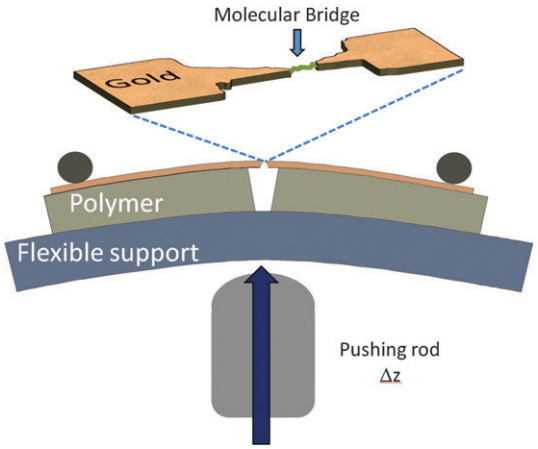

Fig. 2 Schematic diagram of a mechanically controlled break junction (MCBJ).

mechanically controlled break junctions (MCBJs) was coined to describe this setup and they demonstrated that the junction resistance could be adjusted over nine orders of magnitude, from 1 to 10^9 Ω.[32]

A schematic diagram of a MCBJ is shown in Fig. 2. The aim is to form a fine metal bridge that is subsequently cleaved upon bending the whole assembly. Original designs employed a notched metal wire which is mounted using epoxy resin onto an insulated elastic substrate that serves as a bending beam; polyimide films on phosphorus bronze or sprung steel beams have been shown to perform well.[33] The beam is bent and the notched wire cleaved by a pushing rod arrangement in contact with the lower side of the beam. More recently, the design of MCBJs has been refined by the use of microfabrication techniques to define suspended metallic bridges.[33,34] For instance, metallic bridge structures have been lithographically defined on the polyimide layer, which is under-etched in the bridge region by a reactive ion beam to produce a freely suspended bridge.[7,33,35] Such set-ups have a large displacement ratio ($\Delta d/\Delta z$) between the movement of the push rod (Δz) and the displacement of the electrode gap (Δd). $\Delta d/\Delta z$ values of 10^{-4}–10^{-5} are typical making the system very stable against drift and vibrations.[11,33,35] The push rod can be driven by a combination of micrometre screws, stepper motors and/or piezo-elements to achieve the mechanical opening or closing of the gap.

The MCBJ method has been used with great success to form atomic scale metallic constrictions and to examine their electrical and mechanical properties.[33] Notably, the conductance of atomic scale metal contacts has been found to be determined by both quantization of the conductance and the discreteness of the contact size.[36] For gold it has been found that conductance steps near the conductance quantum ($G_0 = 2e^2/h$) prevail at the last conductance step as atomic scale gold contacts are pulled apart.[37] Jumps in conductance during pulling of metallic constrictions appear concomitantly with mechanical force relaxations and have been associated with atomic rearrangements of the metallic wire and contact region.[33] These findings were corroborated by a theoretical analysis.[38,39]

An important development during this time towards the objective analysis of nano-electrical junctions was the use of a histogram representation for the analysis of a large number of conductance curves generated during elongation and contraction cycles of metallic nanowires.[36,40,41] Such histogram representations of conductance data (which in this instance showed a tendency to integer multiples of G_0) proved to be later of great significance in objectively analysing the conductance of metal–molecule–metal junctions (see section 2.7) and in identifying single molecule events.

In 1997 Reed *et al.* demonstrated that the MCBJ method lends itself to the formation of metal–molecule–metal junctions.[6] Before mechanical cleavage a notched gold wire was coated with a self assembled monolayer (SAM) of benzene-1,4-dithiol (BDT). Following cleavage, the pair of separated gold contacts was then also coated with the SAM. The contacts were then slowly moved together to form the molecular junction, recognised by the onset of conductance. These seminal experiments demonstrated the possibility of measuring electrical transport involving a small number of molecules (possibly as few as one molecule), although in the absence of an objective statistical analysis the actual number could not be precisely pinpointed. In 1999 Kergueris *et al.* used lithographically generated suspended MCBJs to form gold electrode pairs spanned by 2,2′:5′,2″-terthiophene-5,5″-dithiol molecular bridges.[7] As with the experiments of Reed *et al.*[6] very few molecules were assumed to be involved in transport across the junction, but definitive proof of the number of molecules involved was not obtained. In an attempt to address the issue of the number of spanning molecules contributing to the *I*–*V* response, Weber *et al.* analysed the response of junctions formed with molecules which were either spatially symmetric or asymmetric in their molecular structure (compounds **1** and **2**, respectively, in Fig. 3).[8] They argued that the differential conductance should exhibit marked asymmetry for single molecule junctions of compound **2**, while junctions with many molecules would not, due to averaging over the randomly oriented molecules. Since asymmetric dI/dV curves were obtained for **2**, but symmetric ones for **1**, they inferred that single molecule junctions could be formed and electrically interrogated.[8]

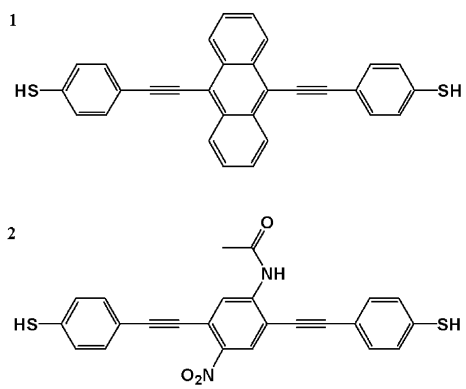

Fig. 3 Molecules used in ref. 8 in MCBJ experiments. Asymmetric dI/dV curves were recorded for **2**, but not **1**, and on this basis it was inferred that single molecule junctions could be formed and electrically interrogated in a MCBJ setup. Thiol end groups are shown as –SH; it is usually thought that the thiol hydrogens are lost on binding to Au.

More recently, metal–molecule–metal junctions formed in MCBJs have been statistically treated through the use of conductance histograms,[9–11] as well as through the statistical analysis of a large set of *I–V* curves recorded during opening and closing of the junction.[42] Using MCBJs and statistically generated conductance histograms, the molecular junction conductance can be examined from G_0 (the metallic point contact) down to $\sim 10^{-7} G_0$, using a logarithmic conductance scale.[10,11] This technique has been used to examine the electrical properties of a range of molecular junctions. It has also been shown that a liquid cell can be introduced into the MCBJ setup,[43] which has enabled electrochemical control to be applied. Broad conductance peaks are seen in the logarithmic conductance histograms of ref. 11, which are nevertheless sensitive to the molecular structure in a rational manner (see for instance the study of a range of conducting oligomers[11]). The broadness of the histogram features has been attributed to fluctuations in the molecular junction.[11]

2.2 Monolayer matrix isolation

Cui *et al.*[2] have developed a method for determining single molecule conductance which relies on isolating the target molecules (typically dithiols with gold contacts) at high dilution in a relatively poorly conducting self-assembling monolayer matrix of alkanethiols on the gold substrate (hence the term "monolayer matrix isolation", MMI). Gold nanoparticles are attached to the free terminal thiol group and the conductance of the whole junction is measured by "touching" the nanoparticle with the conducting probe (either a conducting AFM tip or an STM tip), as illustrated in Fig. 4.

The dithiol molecule forms a chemical contact with the nanoparticle, while the monothiols do not, and the electrical response is dominated by current flow through the nanoparticles and the attached dithiolated molecular bridge. Statistical analysis of the data using histogram plots has shown that the conductance values (G) group themselves into discrete values which are integer multiples of a lowest value. The lowest conductance peak in the histogram (G_1) has been attributed to junctions involving a single molecule. Fig. 5 shows current data as an STM tip is brought down onto a particle resulting in a current jump (marked I_w). The target molecule is hexanedithiol in a 1000 : 1 dilution in a hexanethiol matrix.

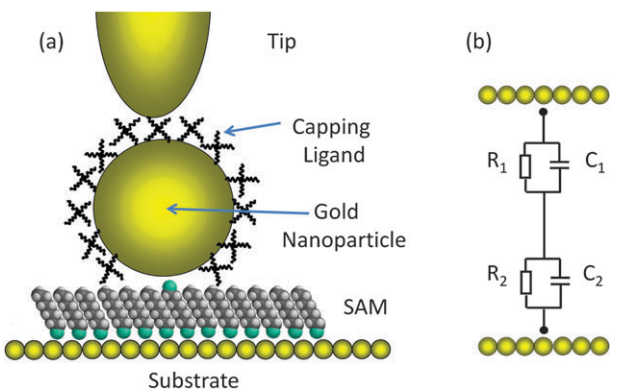

Fig. 4 (a) The "monolayer matrix isolation" method of Cui *et al.*[2] **(b)** The corresponding electrical equivalent circuit.

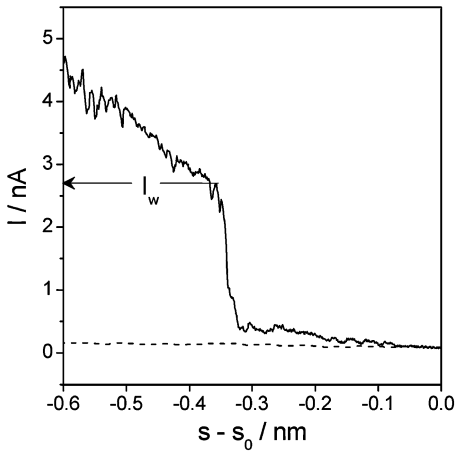

Fig. 5 The matrix isolation method. Current data recorded as an STM tip is brought vertically down onto a particle resulting in a current jump (marked as I_w). The tip is moved from $s - s_0 = 0$ (where s_0 is the initial distance) towards the surface (negative distance values). A control curve obtained on a terrace region is also shown (dashed line). The target molecule is hexanedithiol in a 1000 : 1 dilution in a hexanethiol matrix.

A control curve obtained on a terrace region is also shown. A large number of such jumps are analysed (typically randomly choosing different nanoparticles) and the current jump data is then collected together in histograms of the current (or conductance) jumps.

There are a number of issues that need to be considered when applying this technique. In the original work, Cui *et al.* assumed a metal-to-metal contact between nanoparticle and conducting atomic force microscope tip.[2] In subsequent publications, the intervening capping ligands illustrated in Fig. 4 have been taken into account.[44] If the capping ligand on the gold nanoparticle prevents metallic contact between the gold nanoparticle and tip, the electrical properties of this interface have to also be considered. A simple equivalent circuit is shown in Fig. 4b, with R_1 and C_1 being the resistance and capacitance between tip and nanoparticle, and R_2 and C_2 the resistance and capacitance between the nanoparticle and substrate. For the smaller particles, such as the 1.5 nm phosphine-protected examples used in the original work of Cui *et al.*,[2] the junction acts as a Coulomb blockade and a significant Coulomb blockade region is seen around zero bias. In such cases, when determining R_2 (the desired molecular resistance) the equivalent circuit approximation shown in Fig. 4b has to be considered, otherwise the errors in R_2 are very large. However, if nanoparticles are chosen to be sufficiently large (> 5 nm; ref. 44), the corrections due to Coulomb blockage effects are much smaller. The smaller particles (1.5 nm) also show evidence of quantum size effects, with discrete electronic levels with a spacing of $\sim$0.1 V becoming apparent; the larger particles do not suffer this further complication for room temperature measurements. If a conducting AFM tip is used as an electrical probe in contact mode then deformation of the SAM layer should also be considered.[44,45] This can be very significant for the forces commonly used in contact mode experiments, but has been corrected for by using a mechanical deformation model.[44,45]

2.3 *In situ* break junctions formation

The *in situ* break junction technique was introduced by Xu and Tao in 2003.[1] In this method, break junctions are mechanically formed using an STM tip to create a metallic contact to the substrate, which is then cleaved. As such, the *in situ* BJ technique is conceptually related to the MCBJ methods described in the preceding section. Fig. 6 illustrates the *in situ* BJ method. The STM tip is pushed into the substrate surface to form the metal–metal contact. The tip is then rapidly retracted while monitoring the current. Large current jumps with conductance values corresponding to G_0 (or multiples) occur upon cleavage of the metal contact. This is then followed by smaller current steps as molecular junctions are broken. The metallic wire can be broken in a solution of the target molecules, which then freely adsorb across the gap, or the molecular bridges can be formed from adsorbed molecules preassembled on the surface.

Important parameters for the *in situ* BJ technique include bias voltage, penetration depth of the metal tip into the metal substrate and the retraction speed of the tip from the substrate. The influence of the latter parameter has been described by Huang *et al.*[46] They identified that the degree to which the junction could be stretched prior to junction cleavage depended on the stretching rate.[46] It was found that the stretching distance of the junction just before cleavage could be predicted by thermodynamic bond-breaking theory.[46] At slow stretching rates spontaneous cleavage was found in which thermal fluctuation caused the bridge to break. On the other hand, at fast stretching rates ("adiabatic region"), the forces exerted by the external pulling of the junction dominate.[46] By comparing the breakdown of molecular junctions with that of Au–Au point contacts (nano-constrictions), they concluded that junctions cleave at Au–Au bonds for thiol contacts. Simultaneous force and current determinations have been made using a conducting AFM to form break junctions.[47] The force required to cleave a molecular junction with thiol anchor group in such an experiment was determined as (1.5 ± 0.2) nN.[47] This corresponds to the force needed to break a Au–Au bond in a freely suspended chain of single gold atoms.[48]

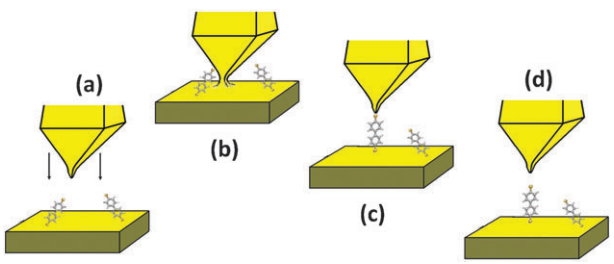

Fig. 6 Schematic illustration of the *in situ* break junction (BJ) method. The tip is directed into the metal surface to establish metal-to-metal contact; (a) to (b). It is then withdrawn until the metallic junction cleaves, between (b) and (c). As the junctions cleaves molecular bridges can form in the gap (c). Following continued retraction of the tip these molecular junctions break themselves (d), producing current jumps that are analysed in histogram plots representing many such cycles.

2.4 The *I*(*s*) technique

Like the *in situ* BJ method described in the preceding section, the *I*(*s*) technique (*I* = current, *s* = distance) introduced by Haiss *et al.* in 2003 also uses an STM to form molecular junctions for electrical measurements.[3] The key difference, however, is in the junction formation method. In the *in situ* BJ method both metal electrodes are pressed together and then this contact is cleaved to form the break junction into which the molecular bridge forms. The *I*(*s*) method, on the other hand, avoids contact between the metal electrodes.[3] The STM tip is brought close to the surface with a low-coverage monolayer of analyte molecules, then withdrawn while the tunnelling current is measured, as shown in Fig. 7. Typically, a gold STM tip and substrate are employed, and in the course of the experiments, one (or a few) molecule(s) forms a junction between tip and substrate, as illustrated schematically in Fig. 7, and the current through the junction is measured.

2.4 The *I*(*t*) technique

A further approach to the determination of single molecule electrical properties using an STM has been developed by Haiss *et al.*[4] As illustrated in Fig. 8, this approach monitors the formation of molecular wires in the time domain and has been referred to as the *I*(*t*) method (*I* = current and *t* = time). The STM tip is placed at constant distance from a low coverage of the dithiol molecule on a Au substrate.[4] This distance is determined by the tunnelling gap resistance and its electronic decay length and it is set to be less than the length of the fully extended molecular junction. Under such conditions, characteristic jumps are observed which appear as telegraphic noise signals. An example *I*(*t*) trace is also shown in Fig. 8. These jumps have been attributed to the attachment or

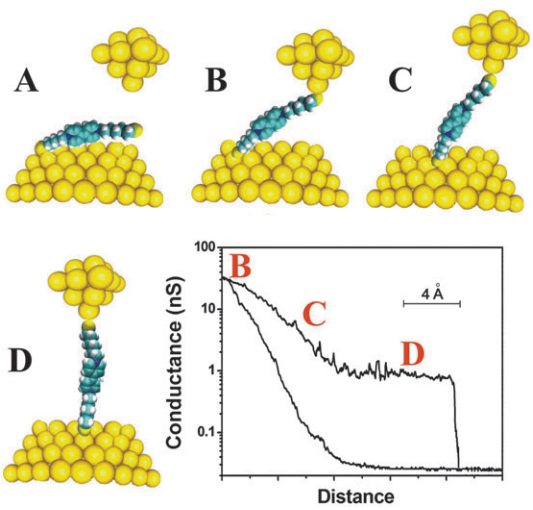

Fig. 7 Schematic illustration of the *I*(*s*) technique; *I* represents current and *s* distance.[3] In this method molecular junctions are formed without first forming metallic break junctions, *i.e.* contact between the STM tip and metallic surface is avoided. As the tip is retracted, the molecular junctions cleave, and these events are statistically analysed in histograms. The graph shows *I*(*s*) curves recorded for the 6-[1′-(6-mercapto-hexyl)-[4,4′]bipyridinium]hexane-1-thiol dication (*6V6*) with the corresponding regions B, C and D marked, together with a decay curve in the absence of molecular bridge formation (lower line).

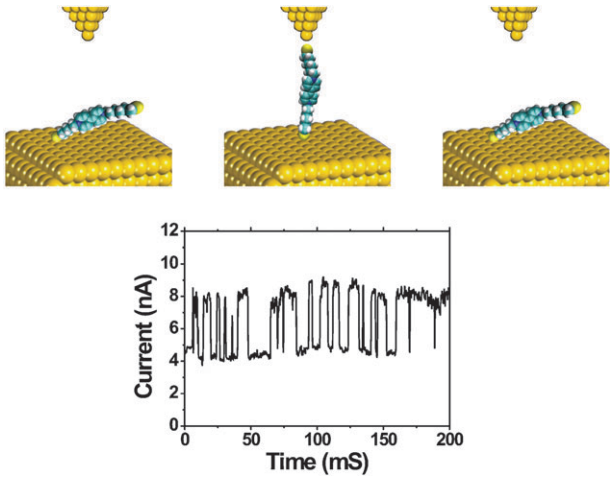

Fig. 8 Schematic representation of the $I(t)$ technique. Molecular junctions stochastically form and break in a constant height gap between STM tip and metal substrate. The junction formation and cleavage process is characterised by current jumps.[4]

detachment of the molecule to or from the STM tip. The conductance of the molecular junction is calculated from the value of the current jumps and the applied tip–substrate bias voltage. Asar *et al*. have provided atomistic simulations of the formation of such molecular junctions.[49,50]

The jumps in $I(t)$ traces are statistically analysed in the form of histogram plots, as previously described for molecular break junctions, in order to distinguish between single molecule and multiple attachment or detachment events. The significance of this technique is its simplicity and its "differential" nature, with differences in current in the presence and absence of a molecule at constant junction separation being measured. This means that through-space tunnelling contributions are minimised, with the current jumps being characteristic then of molecular conductance. The relatively straightforward nature of the telegraphic signals monitored means that the $I(t)$ method lends itself well to automatic detection and analysis of jumps. Haiss *et al*. have described a box car analysis which can be performed on $I(t)$ scans for the automatic detection of the current jumps in the supporting information of ref. 51.

Control experiments are necessary to ensure that the jumps observed can be correctly assigned to molecular events and not to other sources such as instrumental artefacts, noise, and instability in the tip state or surface diffusion. With this in mind, Haiss *et al*. have performed several thousand $I(t)$ scans without data selection in the presence and absence of octanedithiol molecules which can be found in the supporting information of ref. 51. From such control experiments it was concluded that the majority of jumps detected on the octanedithiol covered Au(111) are due to the presence of molecules, with a slight increase in spurious jumps on roughened surfaces. In these control experiments it was found to be important to make $I(t)$ measurements where the tip state was stable (for instance, as judged by the quality of STM imaging). When tip-crashes occurred during data collection, or if the tip was in an unstable state, a quite frequent occurrence of current jumps was noted both in the presence and absence of molecules.[51] Hence $I(t)$ data should only be recorded for well-defined conditions, and conductance values should ideally be corroborated using other methods described in this manuscript.[51]

Xia *et al*. have recently adapted the $I(t)$ method by applying a simultaneous AC modulation to the STM gap separation.[52] This allows the detection of molecular bridge formation, since the AC signal reduces significantly in amplitude when the molecular bridge forms, due to the decreased decay constant for tunnelling through the molecular wire as compared to tunnelling through the solvent. When molecular bridge formation is detected using this AC method a DC current–voltage sweep can then be run to obtain the I–V characteristic for the molecule trapped in the junction. In another recent interesting development Chang *et al*.[53] have used the $I(t)$ method to measure the conductance of gold junctions spanned by a pairing of nucleoside bases interacting by hydrogen bonding.

2.5 Nanofabricated gaps

Conceptually perhaps the simplest method for wiring molecules in metallic junctions is the fabrication of fixed-size metallic gaps with nanometre separation. In practice the fabrication of defined nanometre sized gaps is technically challenging, but it can be achieved using a variety of nanofabrication methods including electron beam lithography with shadow mask evaporation[54] and side etched quantum wells.[55] Using a shadow masking technique at low temperature in UHV gold nanogaps of a few nanometres have been fabricated.[56] Importantly, the ultra low temperature (4 K) froze out the thermal motion of the metal atoms, ensuring that the junction maintained integrity. The two gold electrodes formed source and drain respectively, while an underlying layer of oxidised aluminium on top of an oxidised silicon chip formed a gate electrode.[56] Molecules were introduced in such gaps and during thermal annealing to 70 K thermal mobility allowed the trapping of a molecule in the nanogap.[56] This trapping event was detected by a stepwise increase in junction conductance and the junction was then cooled to 4.2 K with the aim of trapping a single molecule. The three-electrode configuration enabled the determination of single electron transistor characteristics. By changing the gate voltage (V_g), the molecule could be charged to different redox states; in the case of a *p*-phenylenevinylene oligomer containing five benzene rings connected through four double bonds (OPV5), eight redox states were identified and visualised in "diamond plots" in which the source–drain voltage (V_{s-d}) is plotted against V_g in differential conductance maps.[56] This introduction of a gate electrode alongside single molecular junctions, as well as enabling the identification of different molecular states and their influence on transmission, has enabled new aspects of the physics of single molecule devices to be experimentally explored.[56–60] Recently, gate electrodes have been introduced into mechanically controlled break junctions, enabling both molecular gating and fine control of the source–drain distance.[61]

2.6 Nanoparticle–metal–nanoparticle contacts

The fabrication of fixed nano-sized gaps suitable for single molecule devices typically requires separations in the order of

1–3 nm. This can be technically challenging and requires expensive equipment. Dadosh have developed a method which utilises much larger gaps for contacting single molecules.[5] This is achieved by contacting pairs of gold nanoparticles by dithiolated short organic molecules. Dadosh *et al.* have ensured that most of the dimeric gold nanoparticles are bridged by a single molecule by using a large excess of nanoparticles compared to dithiol.[5] The dimeric assemblies are separated from agglomerates containing more than two nanoparticles by centrifugation. 30 nm diameter colloidal gold particles were typically employed and these were introduced into contact gaps of 40–50 nm. This is larger than the size of a nanoparticle and smaller than the dimer length; a schematic diagram of the assembly is shown in Fig. 9. Short organic molecules such as 1,4-benzenedimethanedithiol (BDMT) and 4,4′-biphenyldithiol (BPD) were electrically interrogated in these platforms at low and variable temperatures. Transport features associated with molecules were recognised in differential conductance spectra with BPD and BDMT showing markedly differing electrical behaviour. This method of pre-assembling nanoscale structures containing one or a small number of molecular junctions and then adsorbing these structures in a micro-electronics platform has been taken up by others; for instance gold nanorods have been used for establishing connections to molecules.[62]

2.7 Statistical analysis

As, usually, neither how many molecules form the junction for any given experiment, nor the exact nature of the metal–molecule bonding are known, many measurements are made and the results are analysed statistically to determine the current through a single molecule. The statistical analysis of molecular junctions is similar to that originally developed for the analysis of the conductance of metallic nano-constrictions in the MCBJ method (see section 2.1). Cui *et al.*[2] applied a statistical analysis to examine molecular junctions containing single or a few alkanedithiol molecules in a monothiol matrix. This gave the first clear statistical evidence that electrical measurements could be made on single molecules. They found that current–voltage curves were ''quantised'' as integer multiples of a fundamental curve.[2] These current–voltage curves were related as integer multiples of one another by plotting histograms of a divisor (X) which was chosen to minimise the variance between any given curve and the fundamental I–V curve with $X = 1$. This histogram analysis showed sharp peaks at integer multiples of X, with $X = 1$ being used to identify single molecule junctions.[2]

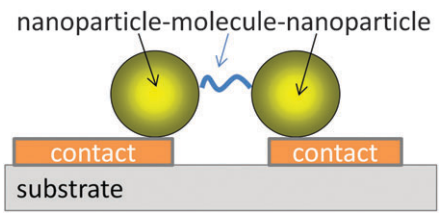

Fig. 9 An illustration of the immobilisation of a gold nanoparticle–molecule–gold nanoparticle conjugate within a micro-electronics assembly for the determination of single molecule electrical properties.[5]

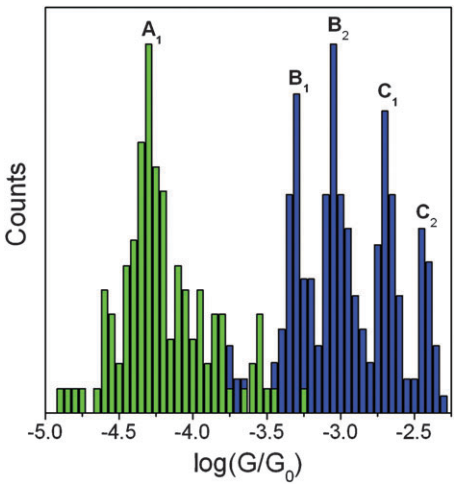

Fig. 10 Logarithmic conductance histograms of pentanedithiol PDT on Au(111) obtained using the $I(s)$ method (green); $U_0 = 0.6$ V; $I_0 = 10$–20 nA; 121 scans have been analysed in total. A logatithmic conductance histogram of PDT on Au(111) obtained using the BJ method is shown in blue; $U_0 = 0.6$ V; $I_0 = 20$ nA; 228 scans have been analysed in total.

Histograms have also been used to analyse current–distance curves generated by the *in situ* BJ method, $I(s)$ method, $I(t)$ method and also MCBJs. Fig. 10 shows, for illustration, histograms obtained by the $I(s)$ method for pentanedithiol (PDT) on Au(111) in green on a logarithmic scale. This histogram exhibits only one peak marked as A_1. Also shown in Fig. 10 in blue is a conductance histogram observed with the BJ technique which exhibits four conductance peaks marked as B_1, B_2, C_1 and C_2. Possible causes of the differing conductance groups are discussed in the following section. Histograms like the one in Fig. 10 are generated by directly determining the height of each current jump in the current–distance scans and plotting these values in histograms of counts against current (or conductance) jump value. This generates one conductance value per jump-containing current–distance scan. Alternatively, histograms can be presented which contain all the current values acquired during a current–distance curve. Both methods can be considered as complementary and have yielded the same conductance values and groups for model systems such as octanedithiol.[4,26,51,63] The generation of defined peaks in ''all-current'' histograms relies on there being a relatively flat current-plateau region before the junction is cleaved. This seems to be the case for most molecular junctions studied and published to date. However, a proportion of current–distance curves may show jumps without an extended plateau and as such do not contribute positively to the all current analysis; indeed their contribution is often detrimental since they add to the background or noise in the histogram. A selection method can be useful to distinguish plateau-forming I–s curves from those which have no plateau, with only the former then being co-added to form histograms.[63]

2.8 Multiple conduction groups

A quandary in early single molecule conductance measurements of ''model'' alkanethiol molecular junctions was the

differing values of conductance measured for the same molecule. For instance, Xu *et al.*[1] measured a conductance of 20 nS for octanedithiol using the BJ technique while Haiss *et al.*[4] measured a value of 1 nS for the same molecule. Both methods used gold contacts and involved stretching the molecular junction until cleavage, so this difference was surprising for methods of seeming similarity. Haiss *et al.* showed that both high and low current steps could be observed with the BJ method, and tentatively suggested that the difference between the two values was related to different contact configurations (at the Au–sulfur contacts).[4] More detailed studies later on showed the incidence of several conductance groups which have been named A, B and C or low, medium and high.[26,51,63,64] There has been some disagreement in the literature concerning the origin of these differing conductance groups; they have been attributed to differing contact morphologies between sulfur head groups and gold contacts or to different conductance values for *gauche* and *anti* conformation of the alkanedithiol chain in the contact junction.[26,51,63,64] Some of the most recent experimental evidence for the origin of the differing conductance groups comes from Haiss *et al.*[51] They measured histograms for octanedithiol on gold substrates with different roughness values. In the statistical analysis of the data they found that varying the roughness of one of the contacts had a profound influence on the relative height distribution of histogram peaks.[51] This is illustrated in Fig. 11, which shows that the relative occurrence of B and C groups compared to A is higher on rough as compared to flat surfaces.

On the basis of the observation that the different conductance groups could be related to differing surface roughness, it was proposed that the differing groups could be related to differing coordination of the sulfur head group, with the higher groups involving adsorption at step edges or similar high coordination sites (*e.g.* gold adatoms) as illustrated in Fig. 12.[51] This notion was corroborated by statistical analysis of the distance at which the molecular junction cleaved to give current steps in the $I(s)$ traces, with $s_A > s_B > s_C$ (Fig. 12). Adsorption of the sulfur head-group at step edges as compared to adsorption on flat surface areas may increase the junction conductance due to mechanical stabilisation of the contact and due to an increase

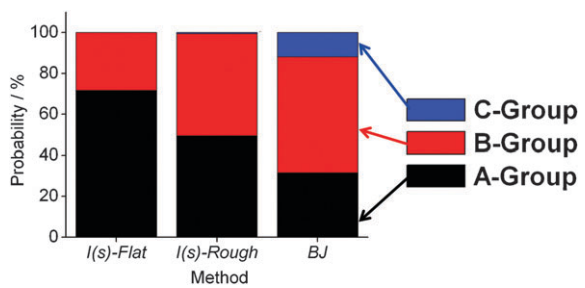

Fig. 11 A representation of the distribution of conductance groups (A, B, C) of the $I(s)$ technique on flat terraces of Au(111) surfaces ($I(s)$-flat), the $I(s)$ technique on rough surfaces ($I(s)$-rough) and the break junction (BJ) technique. The bar chart diagram shows the A, B and C (low, medium, high) conductance ratios for these three different experiments. For a further description of the $I(s)$ measurements on flat Au(111) terraces ($I(s)$-flat) or rougher surface regions ($I(s)$-rough) see ref. 51.

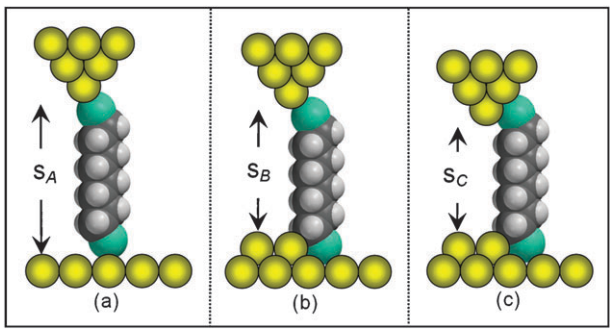

Fig. 12 Three possible configurations of an octanedithiol molecular bridge between a pair of gold contacts: (a) shows both sulfur atoms coordinated to either single gold atoms or terrace sites; (b) on the other hand shows the bottom thiolate contact in a more highly coordinated step site; while (c) shows both thiolate contacts adsorbed in high coordination defects. The tip–sample distances s_A, s_B, s_C marked in the Figure are in good agreement with the distances which have been experimentally determined in ref. 51 for group A, group B and group C events. Reprinted with permission from ref. 51. Copyright 2009 American Chemical Society.

of the electronic coupling, which would rationalise the increasing conductance from (a)–(c) in Fig. 12.

2.9 Comparison of different methods

The recognition of the occurrence of different conductance groups, whose distribution depends on the manner in which the junctions are repeatedly formed, has helped in reconciling the different methods. Fig. 13 compares conductance values for Au–octanedithiol–Au single molecule junctions formed by different methods. Average conductance values for the different conduction groups are marked as vertical lines (A_1: 0.96 nS; B_1: 3.82 nS; C_1: 17.0 nS). For all the techniques which involve single molecule junctions (*i.e.* all methods except nanopores) the average conductance values lie within the error bars for all of the data points. This indicates good agreement between the different experimental methods, resolving

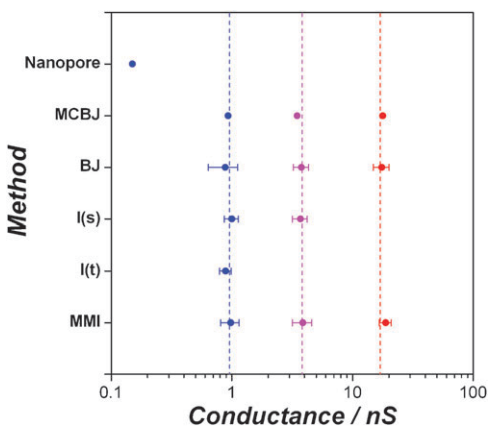

Fig. 13 Comparison of single molecule conductance values for octanedithiol between gold contacts obtained by different methods. The MCBJ data are taken from ref. 66. The nanopores data are from ref. 65, while the $I(s)$ (section 2.4), BJ (section 2.3), $I(t)$ (section 2.4) and MMI (monolayer matrix isolation, section 2.2) data are taken from ref. 51.

the apparent inconsistency in earlier literature that seemed to point to differences in values for different methods.[51] The nanopore data point was calculated from the experimental current density data of Wang *et al.*[65] assuming that the surface area occupied by a single ODT molecule is 0.217 nm^2 which is the area occupied by a single molecule in a $(\sqrt{3} \times \sqrt{3})R30^\circ$ structure on Au(111). The nanopore results obtained on self assembled monolayers clearly exhibit a smaller conductance per molecule as compared to the single molecule experiments, probably arising because not all molecules are connected at both ends due to the roughness of the contacting metal surfaces.

3. Dependence of single molecule conductance on molecular structure, contacts, environment and physical parameters

3.1 Molecular structure and contacts

Using the methods described above it has been possible to study in a systematic fashion the influence of electronic and geometric structure on single molecule conductance. "Chemical" and hence electronic factors that are expected to influence junction conductance include the chemical contact group,[67–69] the redox state of the molecular bridge[3,20,70,71] and chemical substituents on the molecular bridge.[22,72–74] Geometrical factors which influence junction conductance include the conformer distribution,[29,75] the detailed attachment geometry of the molecular headgroups,[51] the intramolecular tilt angles[13] and the contact separation.[14] The intuition from chemical bonding theory is that fully conjugated backbones will give electronically more transmissive junctions than equivalent non-conjugated analogues; indeed, this had been previously demonstrated in photo-physical measurements using donor–bridge–acceptor compounds, using electrochemistry and self assembled monolayers and for large area metal–molecule–metal junctions (see ref. 76 and references therein). There are now many examples of single molecule measurements fulfilling the expectation that conjugated analogues are more transmissive. For instance, using MCBJs Mayor *et al.* have shown that a molecular rod with conjugation broken by a metal centre (*trans*-$[Pt(PPh_3)_2(-C{\equiv}C-C_6H_4SH)_2]$) has several orders of magnitude lower conductance than slightly shorter but well conjugated oligophenylene–ethynylene molecular rods.[77]

Ring substituents in organic molecular wires can have a profound effect on single molecule conductance by shifting frontier molecular orbitals involved in the molecular-junction process. For instance, Li *et al.*[22] have analysed the conductance of substituted oligophenylethylene molecular conductors, with an $-NO_2$ substituent on the central phenyl ring. The $-NO_2$ substituent could in turn be irreversibly electrochemically reduced to give a series of oligophenylethylenes with the substituent X = $-NO_2$, –NO, –NHOH and NH_2; the latter could be protonated to $-NH_3^+$. Using this series of molecules they showed a pronounced influence of the substituent –X on molecular conductance and demonstrated that the conductance decreases linearly with the Hammett *meta*-substituent parameter.[22] A larger Hammett parameter is related to a higher electron withdrawing action of the substituent which was in turn related to the lower conductance measured.[22] A further contribution to experimentally establishing links between electronic structure and conductance has been made by Quinn *et al.*[73] who examined a series of aromatic diamine molecular conductors. They found a good correlation between the molecular conductance measured by the STM-BJ method and the electrochemical oxidation potential, indicating that the HOMO level is responsible for tunnelling transport through these aromatic diamines.[73]

Chemical contacts other than thiol have been investigated with gold electrodes and these have included, for example, 4-pyridyl,[1] S=C=N–R,[78] C≡N–R,[79] N≡C–R,[79] RCO_2^-,[67,69] RCS_2^-,[80] H_2NR,[67,81] RSe^-,[82] $RPMe_2$[81] and even C_{60},[83] although not all of these studies involve *single* molecule measurements. Although thiolate-contacts have provided a strong test-bed for studying the electrical properties of single molecules in electrical junctions, there are a number of potential inadequacies. For instance, high contact resistance is apparent and at ambient temperatures there is substantial mobility at the chemisorbed contacts and the appearance of stochastic switching of the junction conductance.[82,84,85] Much of the earlier focus on the electrical properties of single molecules was centred on the molecule backbone, with the assumption (implicit or explicit) that the metal-terminal group contacts (usually Au–SR) offer comparatively little resistance. Indeed, measurements have been reported on alkanedithiols $HS(CH_2)_nSH$ (n = 6–12) in which, by extrapolating the molecular conductance data back to n = 0, high conductance values for the Au–SR contacts, even approaching the point contact value (77 μS), have been reported.[67,86] However, more recent measurements have shown contact conductance orders of magnitude less than 77 μS, as well as an anomalous length dependence for alkanedithiols with polymethylene chains from C_3 to C_7 in length.[87] Clearly more work is needed to fully shed light on the role of the contact and to provide high transmission, non-labile and chemically robust contacts.

As well as the chemical contacts to the metal electrodes, the separations between the two metal contacts forming the metal–molecule–metal junctions can have a pronounced influence on junction conductance. In particular, short distances between the contacts may lead to the molecule being substantially tilted in the junction. Understanding this influence of the gap separation is an important issue in nano-electronics since nanoelectrode contacts, which may be produced in an electrical device, can show a considerable spread of contact-gap separation. Indeed, any practical molecular electronics device would have to show considerable tolerance to such variability in electrode gap separation in devices. As such, determining the influence of electrode gap spacing is a significant issue in molecular electronics. Haiss *et al.* have demonstrated that the molecular conductance can be measured as a function of contact spacing controlled to sub-nanometre precision.[14] In a more recent study, the effect of the electrode contact gap separation on the electrical properties was also studied for a series of conformationally rigid molecular wires with π-aromatic systems.[15] Data showed the general trend for conductance to increase rather dramatically as the gap between the electrode contacts was closed.[15] DFT computations have illustrated the pronounced influence of tilting molecules

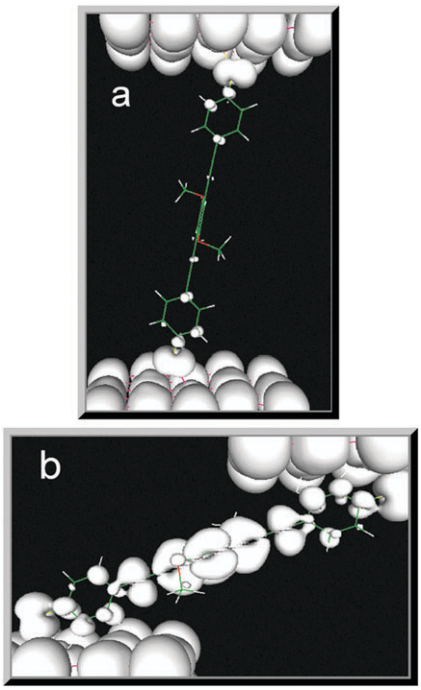

Fig. 14 DFT computed surfaces of constant density of states for a conjugated molecular bridge attached with thiol end groups between a pair of gold contacts. Two different tilt angles are shown: a, $\theta = 10$; b, $\theta = 70^{\circ}$. The tilting leads to greatly increased electronic transmission (molecular conductance). Reprinted by permission from Macmillan Publishers Ltd, *Nature Materials*, ref. 14, copyright 2006.

between two electrodes. Fig. 14 illustrates how the computed electronic transmission through a conjugated molecular bridge increases as it is tilted from 10° (with respect to the surface normal) to 70°.[14] This Figure pictorially shows how the DFT computed surfaces of constant density of states changes on tilting the molecule.

3.2 Temperature dependence

Although the influence of the structure of the molecular bridge on the junction conductance has been studied most widely, the influence of the environment has also been explored to a lesser extent. The influence of temperature, solvent environment and gap separation has been investigated in a number of studies. Temperature is a powerful variable in studies of charge transmission through molecular junctions since it gives access to quantitative determination of charge transport mechanisms. Selzer *et al.* have shown that it is possible to measure the temperature dependence of the current–voltage (*I–V*) response of a single (or small number) of molecules immobilized in an electrical break junction.[28] They showed that electron transport in a π-conjugated molecular bridge could be thermally activated from coherent superexchange tunnelling to incoherent temperature dependent hopping at higher temperatures.[28] As the mechanism of charge transport in simple alkanedithiols is likely to be superexchange, since the frontier orbitals are so far from the Au Fermi energy, no dependence upon temperature would be expected. Surprisingly, however, Haiss *et al.* measured the conductance of a series of alkanedithiols in the temperature range 20–90 °C and found large conductance changes.[29] For instance, the conductance of 1,9-nonanedithiol was found to increase from 0.52 nS at 20 °C to 2.90 nS at 67 °C.[29] This was attributed to the change in distribution between molecular conformers, with the higher energy more folded and *gauche* rich conformers becoming increasingly populated with rising temperature. Through DFT based conductance calculations of a large selection of conformers placed between gold leads Jones and Troisi found the general trend for conductance to increase with conformational energy (for conformational energies >2 kcal mol^{-1}; it should be noted that although the all-*trans* conformer is more conductive than the conformers with the addition of one *gauche* defect, DFT shows that the addition of several *gauche* folds can substantially increase conductance, see ref. 75). These DFT computations rationalise the experimental observation of temperature dependent conductance of alkanedithiol molecular junctions.[75] Kornyshev and Kuznetsov, on the other hand, explained the temperature dependence by showing that the tunnelling conductance in the flexible alkanedithiol is controlled by temperature dependent fluctuations of the relative conformations between nearest neighbour units of the chain molecule.[88] Experimentally, it has also been shown that when flexible chain molecules are stretched in the Au–molecule–Au junction, temperature dependence is quenched; likewise, equivalent rigid molecular bridges[14,30] or alkanes in a self assembled monolayer[57] do not show this temperature dependence.

3.3 Redox state dependence

Electrochemical environments have been particularly rewarding for single molecule conductance studies since they enable the redox state of the molecule and the electrochemical potential drop at the surface to be controlled.[17–25,3] Haiss *et al.* were the first to demonstrate that single molecule conductance can be determined in an electrochemical environment.[3] They showed that the conductance of a Au–molecule–Au junction with the viologen (V^{2+}) molecule **3** (Fig. 15) increased from 0.49 ± 0.08 nS to 2.8 ± 0.8 nS as the molecule was electrochemically switched from the $2+$ to the radical cationic state.[3] In this experiment, changes in the electrochemical potential alter the relative energetic positions of the metal-contact Fermi energy and the molecular electronic levels of the redox group, as schematically illustrated in Fig. 16. This has been referred to as a molecular electrochemical transistor configuration, where the counter or reference electrode may be considered as a gate, while the STM tip and substrate are considered as source and drain.

A striking observation is that the conductance of junctions with **3**, measured either in ambient, or under potential control in the 'off' (V^{2+}) state, is much higher than the conductance of $HS(CH_2)_{12}SH$, *i.e.* two $HS(CH_2)_6$– moieties 'back to back' with no intervening redox group (0.012 nS).[3,17,20,23] This has been interpreted in terms of 'double tunnelling barrier' behaviour.[19] That is, it is easier for electrons to tunnel through two narrow barriers separated by a 'well' (the π-conjugated group) than it is for them to tunnel through one wide barrier. This is analogous to the situation in $Ga_{1-x}Al_xAs$–GaAs–$Ga_{1-x}Al_xAs$ thin film inorganic devices, in which a narrow-bandgap semiconductor is sandwiched between two wider-bandgap semiconductors.

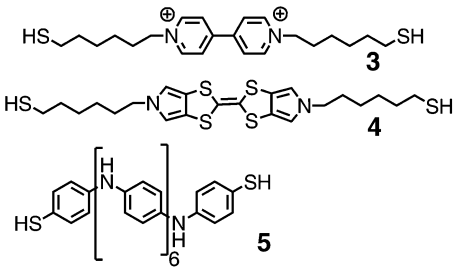

Fig. 15 Viologen (**3**), pyrrolo-TTF (**4**) and oligoaniline (**5**) redox molecules studied respectively in ref. 3, 20 and 89.

Scanning tunnelling spectroscopy (STS) experiments on monolayers of redox-active molecules have previously shown that the tunnelling current through the molecules increases as the redox potential is approached, and then decreases again, in a Gaussian fashion.[23,90–94] Such behaviour has been successfully interpreted in terms of a 2-step electron transfer (ET) model with partial vibrational relaxation at the redox centre developed by Ulstrup, Kuznetzov, *et al.*[95–97] However, it was noted by Haiss *et al.*, and later by Li *et al.*, that the conductance of **3** increased steadily across the $V^{2+}/V^{\bullet+}$ equilibrium potential, and did not then decrease within accessible negative overpotentials. Haiss *et al.*[17] suggested a 'soft gating' mechanism to rationalise this behaviour, in which large configurational fluctuations of the molecular bridge, due to the flexible alkyl linkers in the isolated molecules within the junctions, are responsible for an inhomogeneous broadening of the conductance–overpotential relation that means the system does not behave in the same manner as redox-active molecules in self-assembled monolayers in STS experiments. Li *et al.*[22] examined **3** using a modified $I(s)$ technique and found similar behaviour, albeit with a smaller increase in conductance in the 'on' state. They also carried out STS studies on close-packed monolayers of an analogue of **3** with a single thiol contact,[22,71] and found that, in this case, there was indeed a peak in the conductance-overpotential relation, which is in agreement with the 'soft' gating concept. Interestingly, however, Leary *et al.*[27] later carried out $I(s)$ experiments under electrochemical control on molecule **4**, and found here that, even in single molecule Au–**4**–Au junctions, the conductance rises as the $\mathbf{4}/\mathbf{4}^{+\bullet}$ redox potential is reached, and then falls at positive overpotentials (Fig. 16). They tentatively suggested that the reason may lie in the fact that, whereas V^{2+} molecules are twisted, but $V^{\bullet+}$ have coplanar rings owing to the larger C=C character of the inter-ring bond, the pyrrolo-TTF group has coplanar rings in both its neutral and $^{\bullet}+$ states. This will make solvent reorganisation effects relatively more important for **4**, which will tend to make the system behave more classically.

Thiol-terminated oligoaniline **5** likewise showed a peak in its conductance as a function of potential.[89] The conductance of junctions involving the neutral (leucoemeraldine) **5** in toluene was 0.32 ± 0.03 nS, but under electrolyte (0.05 M H_2SO_4), the partially–protonated, half-oxidised (emeraldine) junctions gave a low-bias (U_{tip} −0.05 V) conductance of 5 nS.[89] Here,

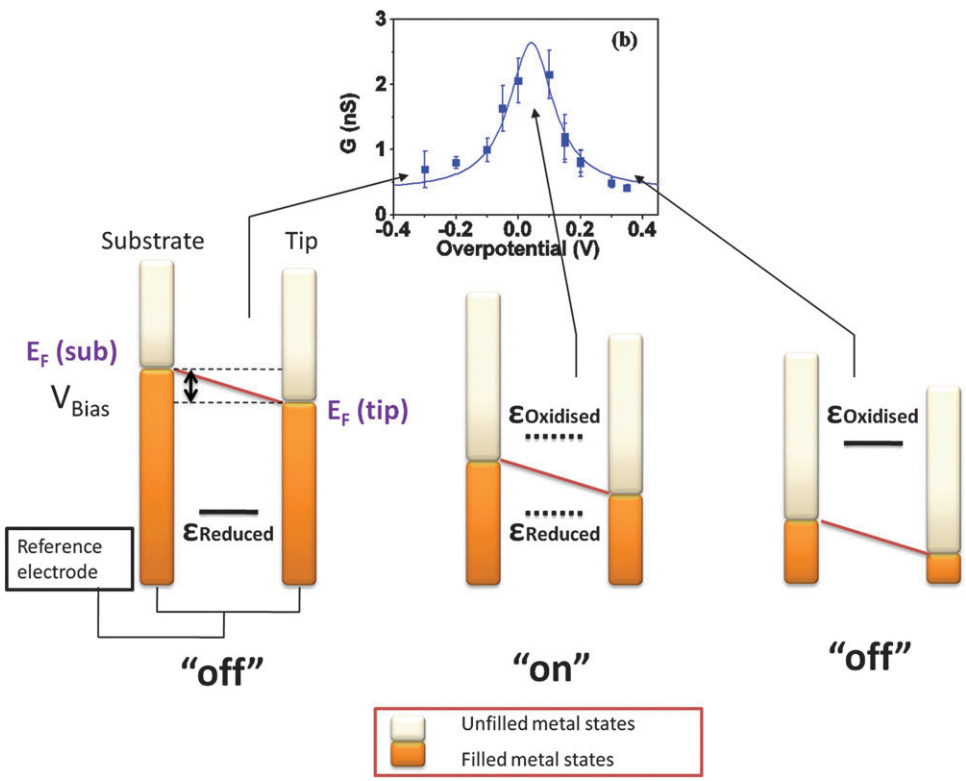

Fig. 16 Schematic illustration of the operation of a redox-active metal–molecule–metal junction. The energy of the frontier orbital will be different in the two redox states ('$\varepsilon_{Oxidised}$' and '$\varepsilon_{Reduced}$') owing to bond length changes and solvent reorganization on electron transfer. In the 'off' states, the corresponding orbitals are both far from the contact Fermi energies, either below (left) or above (right).

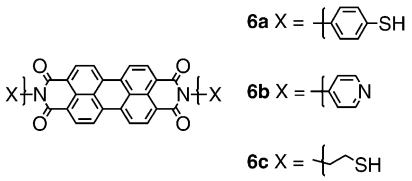

Fig. 17 Rigid, conjugated redox molecules **6a**, **6b** and **6c** studied in ref. 24.

too, the low-bias conductance reaches a maximum when the oligomer is in its 'emeraldine salt' (*i.e.* half-oxidised) state. Interestingly, in this case the molecule showed bias-dependent conductance, the conductance falling from 5 nS at $U_{tip} = -0.05$ V to 1 nS at -0.2 V.

The more rigid and conjugated redox-active molecules **6** (Fig. 17) have been studied by Li *et al.* using the STM-based break junction method.[24] The reduction of the perylene tetracarboxylicdiimide (PTCDI) moieties was only just accessible before reductive thiol desorption occurred, so although the conductance of the Au–**6**–Au junctions as a function of potential in this system showed a steady increase as the redox peak was approached, one cannot conclude that the system behaves like the viologen molecule **3**. In fact, junction current *vs.* gate voltage experiments on individual junctions with **6a** showed some evidence for a peak in conductance.[24] These molecules showed a bigger increase of conductance upon reduction than for **3–5**; over two orders of magnitude for **6a**.[22] Temperature dependence measurements were consistent with thermally-activated conductance and a two-step ('hopping') mechanism for the 'off' state, but there was no temperature dependence for the reduced ('on') state.[24] Cao *et al.* used a combination of molecular dynamics simulations and transport calculations to probe theoretically the temperature dependence of the 'off' state conductance.[98] They proposed that the H-bonding of water molecules to the carbonyl oxygens is disrupted at higher temperature, causing changes in the statistical behaviour of the conductance of the junctions that broaden the conductance histograms and shift the mean conductance to a higher value.[98]

3.4 Medium effects on single molecule conductance

Long *et al.* measured the electrical properties of self-assembled monolayers bound to gold through thiols, using a technique in which a gold-on-nickel-coated silica colloid particle is magnetically oriented between two gold contacts bearing self-assembled upright-standing thiol or dithiol monolayers.[99] They found that the presence of water lowered the conductance of their junctions by approximately half an order of magnitude per Au–S bond in the junction, and they published spectroscopic data supporting the idea that reversible hydration of the Au–S bond was responsible for the lower conductance.[99] However, extensive single molecule conductance experiments on α,ω-alkanedithiols have shown that the conductances of metal–single molecule–metal junctions with these simple molecules are not significantly affected by solvent environment. van Zalinge *et al.*,[100] Li *et al.*,[26] and others have studied these molecules under hydrocarbons (*e.g.* dodecane, mesitylene), fluorocarbons, aqueous electrolytes and UHV, and the conductance values (taking into account the existence of the three conductance groups; section 2.9) for a given molecule are the same within experimental error.

In intermolecular or intramolecular electron transfer, it is a tenet of Marcus theory that reorganisation of the solvent medium can play a key role in controlling the rate. Recently, the first example of a very large effect of the medium upon the conductance of metal–single molecule—metal junctions was noted.[27] The conductance of Au–molecule–Au junctions with the series of molecules **7a–d** (Fig. 18) was measured by Leary *et al.*[27] using the *I*(*s*) method, as part of ongoing work to probe further the validity of the concept of 'organic double tunnelling barrier' molecules. It might be expected that since the length of these molecules increases from **7a** to **7d**, and as they conduct by superexchange, the conductance should fall exponentially with length. Offsetting this, however, the π and π* frontier orbitals would be expected to be closer to the contact Fermi energy as conjugation increases from **7a–7d**, and this might increase conductance. In fact, it was found that the conductance increased significantly from **7a** to **7b**, and then remained essentially constant at *ca.* 1 nS (Fig. 18, left panel; red line).[27]

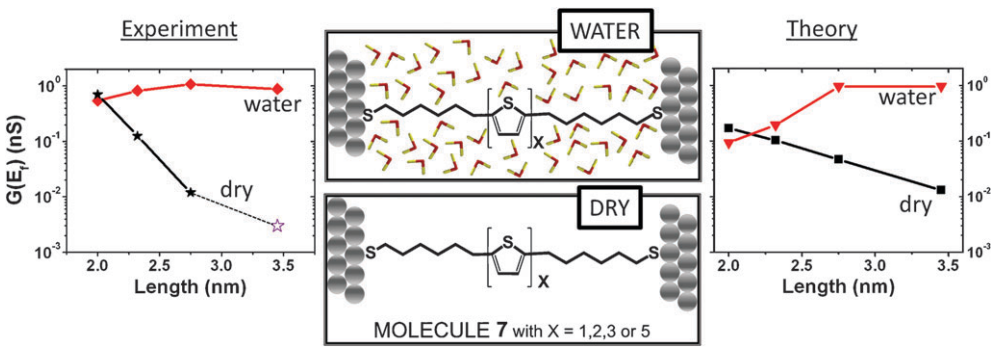

Fig. 18 Experimental (left) and theoretical (right) results for the single molecule conductance of **7a–d** in water and in the absence of water.[27] The central pictures illustrate the oligothiophene (**Molecule 7** with $x = 1$ (**7a**), 2 (**7b**), 3 (**7c**), 5 (**7d**)) molecular bridge between gold contacts. For $x = 3$, the presence or absence of environmental water changes the conductance **by two orders of magnitude**. Theory reveals that H_2O significantly increases the conductance of the longer molecules (**7c**, **7d**; $x = 3, 5$) by interacting with the π orbitals of the thiophene rings and shifting orbital energies, such that the frontier orbitals move closer to the Au Fermi energy. By cycling between 'wet' and dry argon the conductance for **7c** could be changed reversibly.

Transport calculations using the non-equilibrium Green's function SMEAGOL approach, however, predicted that the conductance should decrease exponentially from **7a** to **7d**, (Fig. 18, right panel; black line).[27] It was realised that the difference between experiment and theory is that the calculations assume that the junction is in a vacuum, whereas the measurements were carried out in ambient conditions. The behaviour of the oligothiophene 'core' in the presence of water was examined theoretically. The most stable water–thiophene interaction was found to be that of the positively charged H atoms of water with the thiophene ring π-system. When transport calculations were repeated with bound waters interacting with the thiophene rings in this fashion, the transport resonances were shifted, such that for the longer oligothiophenes, the conductance of the junctions substantially increased (Fig. 18, right panel; red line), almost in complete agreement with the experiment.

This prompted us to repeat the $I(s)$ measurements on **7a-d** using a dry argon atmosphere.[27] The results are indicated in Fig. 18, left panel (black line); note that the value for the quinquethiophene molecule, **7d**, is an upper limit, since we were unable to measure a conductance value for this molecule in the absence of water, as the tunnelling currents lay below the limit of our most sensitive current follower. The slope of this line is larger than for the calculated values; this may be a consequence of the use of the local density approximation for the DFT calculations, which may exaggerate the effect of greater conjugation.

4. Summary

The study of single molecule electronics has rapidly expanded in a relatively short period of time. It is now possible to reliably measure single molecule electrical properties such as molecular conductance, complete current–voltage response and single molecule transistor characteristics in electrochemically gated or 3-terminal measurements. A number of competing and complementary techniques are available, which despite earlier quandaries have shown consistent values for model systems such as alkanedithiols. Techniques such as "monolayer matrix isolation",[2] MCBJs,[6–11] *in situ* BJs[1] and the $I(s)$ method[3] are now been used by a growing number of groups in research labs worldwide to study a wide variety of single molecule junctions. For these techniques, statistical analysis of molecular conductance data in the form of histograms has been most important in the reliable interpretation of data. On the other hand, detailed electrical information has been obtained for nanofabricated devices where molecular junctions can be "frozen" at ultra-low temperatures and detailed electrical characteristics can be recorded (*e.g.* Coulomb diamond plots).[56–60]

Single molecule electrical methods have enabled structure–property relationships to be determined and intricate aspects of device physics to be examined. In many cases, single molecule electrical behaviour mirrors that of extended molecular films. In other cases, phenomena not identified or observable for molecular films and multi-molecular devices have become apparent at the single molecule level. Examples include the unexpected temperature dependence of alkanedithiols,[29,30,75,88] molecular contact effects and the occurrence of multiple conductance groups,[26,51,63,64] single molecule charging and Kondo phenomena and single molecule transistor behaviour.[3,17,20,23,56,60,90–94]

The advances made in the experimental determination of single molecule electrical characteristics have been accompanied by significant advances in theory. *Ab initio* electronic transport codes based on implementations of density functional theory (DFT), combined with for instance non-equilibrium Green's function transport methods, have been rather widely used for describing two-terminal devices incorporating single molecules.[101–103] Issues related to the inadequacies of mean field theories based on DFT and the need to take into account molecular charging energies and screening from the metal contacts have been discussed in recent literature.[104–107] Recognising the dynamic nature of molecular junctions at room temperature, computational studies have been performed over many differing junctions geometries[108] or in the case of conformationally flexible molecules for many conformations.[75] The influence of molecular tilting on the electronic transmission has also been theoretically addressed.[14] Many single molecule electrical measurements are performed in condensed media such as water, electrolytes or organic media and recent studies have taken steps in introducing the environment within computational frameworks.[27,98]

The ability to make reliable single molecule electrical measurements from ultra-low temperature UHV environments to ambient temperature electrochemical conditions has given great impetus to the field of molecule electronics. It is expected that such fundamental studies will contribute to the development of new paradigms in molecular electronics, both in terms of designing new functional molecular structures as well as contacting and addressing strategies. An important future direction would be single molecule measurements on device relevant molecular structures and contacts, which would include semiconductor and low resistance electrical contacts to molecules. The further development of ac methods[52] for the determination of molecular electrical characteristics would also be of significance.

References

1 B. Q. Xu and N. J. J. Tao, *Science*, 2003, **301**, 1221–1223.
2 X. D. Cui, A. Primak, X. Zarate, J. Tomfohr, O. F. Sankey, A. L. Moore, T. A. Moore, D. Gust, G. Harris and S. M. Lindsay, *Science*, 2001, **294**, 571–574.
3 W. Haiss, H. van Zalinge, S. J. Higgins, D. Bethell, H. Hobenreich, D. J. Schiffrin and R. J. Nichols, *J. Am. Chem. Soc.*, 2003, **125**, 15294–15295.
4 W. Haiss, R. J. Nichols, H. van Zalinge, S. J. Higgins, D. Bethell and D. J. Schiffrin, *Phys. Chem. Chem. Phys.*, 2004, **6**, 4330–4337.
5 T. Dadosh, Y. Gordin, R. Krahne, I. Khivrich, D. Mahalu, V. Frydman, J. Sperling, A. Yacoby and I. Bar-Joseph, *Nature*, 2005, **436**, 677–680.
6 M. A. Reed, C. Zhou, C. J. Muller, T. P. Burgin and J. M. Tour, *Science*, 1997, **278**, 252–254.
7 C. Kergueris, J. P. Bourgoin, S. Palacin, D. Esteve, C. Urbina, M. Magoga and C. Joachim, *Phys. Rev. B: Condens. Matter Mater. Phys.*, 1999, **59**, 12505–12513.
8 H. B. Weber, J. Reichert, F. Weigend, R. Ochs, D. Beckmann, M. Mayor, R. Ahlrichs and H. von Lohneysen, *Chem. Phys.*, 2002, **281**, 113–125.
9 R. H. M. Smit, Y. Noat, C. Untiedt, N. D. Lang, M. C. van Hemert and J. M. van Ruitenbeek, *Nature*, 2002, **419**, 906–909.

10 M. T. Gonzalez, S. M. Wu, R. Huber, S. J. van der Molen, C. Schonenberger and M. Calame, *Nano Lett.*, 2006, **6**, 2238–2242.
11 R. Huber, M. T. Gonzalez, S. Wu, M. Langer, S. Grunder, V. Horhoiu, M. Mayor, M. R. Bryce, C. S. Wang, R. Jitchati, C. Schonenberger and M. Calame, *J. Am. Chem. Soc.*, 2008, **130**, 1080–1084.
12 N. J. Tao, *Nat. Nanotechnol.*, 2006, **1**, 173–181.
13 L. Venkataraman, J. E. Klare, C. Nuckolls, M. S. Hybertsen and M. L. Steigerwald, *Nature*, 2006, **442**, 904–907.
14 W. Haiss, C. S. Wang, I. Grace, A. S. Batsanov, D. J. Schiffrin, S. J. Higgins, M. R. Bryce, C. J. Lambert and R. J. Nichols, *Nat. Mater.*, 2006, **5**, 995–1002.
15 W. Haiss, C. S. Wang, R. Jitchati, I. Grace, S. Martin, A. S. Batsanov, S. J. Higgins, M. R. Bryce, C. J. Lambert, P. S. Jensen and R. J. Nichols, *J. Phys.: Condens. Matter*, 2008, **20**, 374119.
16 M. S. Hybertsen, L. Venkataraman, J. E. Klare, A. C. Walley, M. L. Steigerwald and C. Nuckolls, *J. Phys.: Condens. Matter*, 2008, **20**, 374115.
17 W. Haiss, T. Albrecht, H. van Zalinge, S. J. Higgins, D. Bethell, H. Hobenreich, D. J. Schiffrin, R. J. Nichols, A. M. Kuznetsov, J. Zhang, Q. Chi and J. Ulstrup, *J. Phys. Chem. B*, 2007, **111**, 6703–6712.
18 W. Haiss, R. J. Nichols, S. J. Higgins, D. Bethell, H. Hobenreich and D. J. Schiffrin, *Faraday Discuss.*, 2004, **125**, 179–194.
19 W. Haiss, H. van Zalinge, H. Hobenreich, D. Bethell, D. J. Schiffrin, S. J. Higgins and R. J. Nichols, *Langmuir*, 2004, **20**, 7694–7702.
20 E. Leary, S. J. Higgins, H. van Zalinge, W. Haiss, R. J. Nichols, S. Nygaard, J. O. Jeppesen and J. Ulstrup, *J. Am. Chem. Soc.*, 2008, **130**, 12204–12205.
21 X. Y. Xiao, D. Brune, J. He, S. Lindsay, C. B. Gorman and N. J. Tao, *Chem. Phys.*, 2006, **326**, 138–143.
22 X. L. Li, B. Q. Xu, X. Y. Xiao, X. M. Yang, L. Zang and N. J. Tao, *Faraday Discuss.*, 2006, **131**, 111–120.
23 Z. Li, B. Han, G. Meszaros, I. Pobelov, T. Wandlowski, A. Blaszczyk and M. Mayor, *Faraday Discuss.*, 2006, **131**, 121–143.
24 X. L. Li, J. Hihath, F. Chen, T. Masuda, L. Zang and N. J. Tao, *J. Am. Chem. Soc.*, 2007, **129**, 11535–11542.
25 N. J. Tao, *J. Mater. Chem.*, 2005, **15**, 3260–3263.
26 X. L. Li, J. He, J. Hihath, B. Q. Xu, S. M. Lindsay and N. J. Tao, *J. Am. Chem. Soc.*, 2006, **128**, 2135–2141.
27 E. Leary, H. Hobenreich, S. J. Higgins, H. van Zalinge, W. Haiss, R. J. Nichols, C. M. Finch, I. Grace, C. J. Lambert, R. McGrath and J. Smerdon, *Phys. Rev. Lett.*, 2009, **102**, 086801.
28 Y. Selzer, M. A. Cabassi, T. S. Mayer and D. L. Allara, *J. Am. Chem. Soc.*, 2004, **126**, 4052–4053.
29 W. Haiss, H. van Zalinge, D. Bethell, J. Ulstrup, D. J. Schiffrin and R. J. Nichols, *Faraday Discuss.*, 2006, **131**, 253–264.
30 S. Martin, F. Giustiniano, W. Haiss, S. J. Higgins, R. J. Whitby and R. J. Nichols, *J. Phys. Chem. C*, 2009, **113**, 18884–18890.
31 J. Moreland and J. W. Ekin, *J. Appl. Phys.*, 1985, **58**, 3888–3895.
32 C. J. Muller, J. M. Vanruitenbeek and L. J. Dejongh, *Physica C*, 1992, **191**, 485–504.
33 N. Agrait, A. L. Yeyati and J. M. van Ruitenbeek, *Phys. Rep.*, 2003, **377**, 81–279.
34 C. Zhou, C. J. Muller, M. R. Deshpande, J. W. Sleight and M. A. Reed, *Appl. Phys. Lett.*, 1995, **67**, 1160–1162.
35 J. M. vanRuitenbeek, A. Alvarez, I. Pineyro, C. Grahmann, P. Joyez, M. H. Devoret, D. Esteve and C. Urbina, *Rev. Sci. Instrum.*, 1996, **67**, 108–111.
36 J. M. Krans, J. M. Vanruitenbeek, V. V. Fisun, I. K. Yanson and L. J. Dejongh, *Nature*, 1995, **375**, 767–769.
37 G. Rubio, N. Agrait and S. Vieira, *Phys. Rev. Lett.*, 1996, **76**, 2302–2305.
38 H. Mehrez and S. Ciraci, *Phys. Rev. B: Condens. Matter*, 1997, **56**, 12632–12642.
39 H. Mehrez, S. Ciraci, C. Y. Fong and S. Erkoc, *J. Phys.: Condens. Matter*, 1997, **9**, 10843–10854.
40 L. Olesen, E. Laegsgaard, I. Stensgaard, F. Besenbacher, J. Schiotz, P. Stoltze, K. W. Jacobsen and J. K. Norskov, *Phys. Rev. Lett.*, 1995, **74**, 2147–2147.
41 Z. Gai, Y. He, H. B. Yu and W. S. Yang, *Phys. Rev. B: Condens. Matter*, 1996, **53**, 1042–1045.
42 E. Lortscher, H. B. Weber and H. Riel, *Phys. Rev. Lett.*, 2007, **98**, 176807.
43 C. Shu, C. Z. Li, H. X. He, A. Bogozi, J. S. Bunch and N. J. Tao, *Phys. Rev. Lett.*, 2000, **84**, 5196–5199.
44 T. Morita and S. Lindsay, *J. Am. Chem. Soc.*, 2007, **129**, 7262–7263.
45 X. D. Cui, X. Zarate, J. Tomfohr, O. F. Sankey, A. Primak, A. L. Moore, T. A. Moore, D. Gust, G. Harris and S. M. Lindsay, *Nanotechnology*, 2002, **13**, 5–14.
46 Z. F. Huang, F. Chen, P. A. Bennett and N. J. Tao, *J. Am. Chem. Soc.*, 2007, **129**, 13225–13231.
47 B. Q. Xu, X. Y. Xiao and N. J. Tao, *J. Am. Chem. Soc.*, 2003, **125**, 16164–16165.
48 G. Rubio-Bollinger, S. R. Bahn, N. Agrait, K. W. Jacobsen and S. Vieira, *Phys. Rev. Lett.*, 2001, **87**, 026101.
49 J. A. O. Asar, M. M. Mariscal and E. P. M. Leiva, *Electrochim. Acta*, 2009, **54**, 2977–2982.
50 J. A. O. Asar, E. P. M. Leiva and M. M. Mariscal, *Electrochem. Commun.*, 2009, **11**, 987–989.
51 W. Haiss, S. Martin, E. Leary, H. van Zalinge, S. J. Higgins, L. Bouffier and R. J. Nichols, *J. Phys. Chem. C*, 2009, **113**, 5823–5833.
52 J. L. Xia, I. Diez-Perez and N. J. Tao, *Nano Lett.*, 2008, **8**, 1960–1964.
53 S. A. Chang, J. He, L. S. Lin, P. M. Zhang, F. Liang, M. Young, S. Huang and S. Lindsay, *Nanotechnology*, 2009, **20**, 185102.
54 A. Bezryadin, C. Dekker and G. Schmid, *Appl. Phys. Lett.*, 1997, **71**, 1273–1275.
55 R. Krahne, A. Yacoby, H. Shtrikman, I. Bar-Joseph, T. Dadosh and J. Sperling, *Appl. Phys. Lett.*, 2002, **81**, 730–732.
56 S. Kubatkin, A. Danilov, M. Hjort, J. Cornil, J. L. Bredas, N. Stuhr-Hansen, P. Hedegard and T. Bjornholm, *Nature*, 2003, **425**, 698–701.
57 E. A. Osorio, T. Bjornholm, J. M. Lehn, M. Ruben and H. S. J. van der Zant, *J. Phys.: Condens. Matter*, 2008, **20**, 374121.
58 H. S. J. van der Zant, Y. V. Kervennic, M. Poot, K. O'Neill, Z. de Groot, J. M. Thijssen, H. B. Heersche, N. Stuhr-Hansen, T. Bjornholm, D. Vanmaekelbergh, C. A. van Walree and L. W. Jenneskens, *Faraday Discuss.*, 2006, **131**, 347–356.
59 E. A. Osorio, K. O'Neill, N. Stuhr-Hansen, O. F. Nielsen, T. Bjornholm and H. S. J. van der Zant, *Adv. Mater.*, 2007, **19**, 281–285.
60 E. A. Osorio, K. O'Neill, M. Wegewijs, N. Stuhr-Hansen, J. Paaske, T. Bjornholm and H. S. J. van der Zant, *Nano Lett.*, 2007, **7**, 3336–3342.
61 A. R. Champagne, A. N. Pasupathy and D. C. Ralph, *Nano Lett.*, 2005, **5**, 305–308.
62 Q. X. Tang, Y. H. Tong, T. T. Jain, T. Hassenkam, Q. Wan, K. Moth-Poulsen and T. Bjornholm, *Nanotechnology*, 2009, **20**, 245205.
63 C. Li, I. Pobelov, T. Wandlowski, A. Bagrets, A. Arnold and F. Evers, *J. Am. Chem. Soc.*, 2008, **130**, 318–326.
64 M. Fujihira, M. Suzuki, S. Fujii and A. Nishikawa, *Phys. Chem. Chem. Phys.*, 2006, **8**, 3876–3884.
65 W. Y. Wang, T. Lee and M. A. Reed, *Rep. Prog. Phys.*, 2005, **68**, 523–544.
66 M. T. Gonzalez, J. Brunner, R. Huber, S. M. Wu, C. Schonenberger and M. Calame, *New J. Phys.*, 2008, **10**, 065018.
67 F. Chen, X. L. Li, J. Hihath, Z. F. Huang and N. J. Tao, *J. Am. Chem. Soc.*, 2006, **128**, 15874–15881.
68 L. Venkataraman, J. E. Klare, I. W. Tam, C. Nuckolls, M. S. Hybertsen and M. L. Steigerwald, *Nano Lett.*, 2006, **6**, 458–462.
69 S. Martin, W. Haiss, S. Higgins, P. Cea, M. C. Lopez and R. J. Nichols, *J. Phys. Chem. C*, 2008, **112**, 3941–3948.
70 X. Y. Xiao, L. A. Nagahara, A. M. Rawlett and N. J. Tao, *J. Am. Chem. Soc.*, 2005, **127**, 9235–9240.
71 I. V. Pobelovt, Z. H. Li and T. Wandlowski, *J. Am. Chem. Soc.*, 2008, **130**, 16045–16054.
72 L. Venkataraman, Y. S. Park, A. C. Whalley, C. Nuckolls, M. S. Hybertsen and M. L. Steigerwald, *Nano Lett.*, 2007, **7**, 502–506.

73 J. R. Quinn, F. W. Foss, L. Venkataraman and R. Breslow, *J. Am. Chem. Soc*., 2007, **129**, 12376–12377.
74 E. Leary, S. J. Higgins, H. van Zalinge, W. Haiss and R. J. Nichols, *Chem. Commun*., 2007, **38**, 3939–3941.
75 D. R. Jones and A. Troisi, *J. Phys. Chem. C*, 2007, **111**, 14567–14573.
76 M. A. Rampi and G. M. Whitesides, *Chem. Phys*., 2002, **281**, 373–391.
77 M. Mayor, C. von Hanisch, H. B. Weber, J. Reichert and D. Beckmann, *Angew. Chem., Int. Ed*., 2002, **41**, 1183–1186.
78 M. D. Fu, W. P. Chen, H. C. Lu, C. T. Kuo, W. H. Tseng and C. H. Chen, *J. Phys. Chem. C*, 2007, **111**, 11450–11455.
79 M. Kiguchi, S. Miura, K. Hara, M. Sawamura and K. Murakoshi, *Appl. Phys. Lett*., 2006, **89**, 213104.
80 Z. Y. Li and D. S. Kosov, *J. Phys. Chem. B*, 2006, **110**, 9893–9898.
81 Y. S. Park, A. C. Whalley, M. Kamenetska, M. L. Steigerwald, M. S. Hybertsen, C. Nuckolls and L. Venkataraman, *J. Am. Chem. Soc*., 2007, **129**, 15768–15769.
82 S. Yasuda, S. Yoshida, J. Sasaki, Y. Okutsu, T. Nakamura, A. Taninaka, O. Takeuchi and H. Shigekawa, *J. Am. Chem. Soc*., 2006, **128**, 7746–7747.
83 C. A. Martin, D. Ding, J. K. Sorensen, T. Bjornholm, J. M. van Ruitenbeek and H. S. J. van der Zant, *J. Am. Chem. Soc*., 2008, **130**, 13198–13199.
84 Z. J. Donhauser, B. A. Mantooth, K. F. Kelly, L. A. Bumm, J. D. Monnell, J. J. Stapleton, D. W. Price, A. M. Rawlett, D. L. Allara, J. M. Tour and P. S. Weiss, *Science*, 2001, **292**, 2303–2307.
85 G. K. Ramachandran, T. J. Hopson, A. M. Rawlett, L. A. Nagahara, A. Primak and S. M. Lindsay, *Science*, 2003, **300**, 1413–1416.
86 B. Kim, J. M. Beebe, Y. Jun, X. Y. Zhu and C. D. Frisbie, *J. Am. Chem. Soc*., 2006, **128**, 4970–4971.
87 W. Haiss, S. Martin, L. E. Scullion, L. Bouffier, S. J. Higgins and R. J. Nichols, *Phys. Chem. Chem. Phys*., 2009, **11**, 10831–10838.
88 A. A. Kornyshev and A. M. Kuznetsov, *Chem. Phys*., 2006, **324**, 276–279.
89 J. He, F. Chen, S. Lindsay and C. Nuckolls, *Appl. Phys. Lett*., 2007, **90**, 072112.
90 T. Albrecht, A. Guckian, A. M. Kuznetsov, J. G. Vos and J. Ulstrup, *J. Am. Chem. Soc*., 2006, **128**, 17132–17138.
91 T. Albrecht, A. Guckian, J. Ulstrup and J. G. Vos, *Nano Lett*., 2005, **5**, 1451–1455.
92 T. Albrecht, K. Moth-Poulsen, J. B. Christensen, A. Guckian, T. Bjornholm, J. G. Vos and J. Ulstrup, *Faraday Discuss*., 2006, **131**, 265–279.
93 J. D. Zhang, A. M. Kuznetsov, I. G. Medvedev, Q. J. Chi, T. Albrecht, P. S. Jensen and J. Ulstrup, *Chem. Rev*., 2008, **108**, 2737–2791.
94 C. Li, A. Mishchenko, Z. Li, I. Pobelov, T. Wandlowski, X. Q. Li, F. Wurthner, A. Bagrets and F. Evers, *J. Phys.: Condens. Matter*, 2008, **20**, 374122.
95 A. M. Kuznetsov and J. Ulstrup, *J. Phys. Chem. A*, 2000, **104**, 11531–11540.
96 J. Zhang, Q. Chi, A. M. Kuznetsov, A. G. Hansen, H. Wackerbarth, H. E. M. Christensen, J. E. T. Andersen and J. Ulstrup, *J. Phys. Chem. B*, 2002, **106**, 1131–1152.
97 J. D. Zhang, Q. J. Chi, T. Albrecht, A. M. Kuznetsov, M. Grubb, A. G. Hansen, H. Wackerbarth, A. C. Welinder and J. Ulstrup, *Electrochim. Acta*, 2005, **50**, 3143–3159.
98 H. Cao, J. Jiang, J. Ma and Y. Luo, *J. Am. Chem. Soc*., 2008, **130**, 6674–6675.
99 D. P. Long, J. L. Lazorcik, B. A. Mantooth, M. H. Moore, M. A. Ratner, A. Troisi, Y. Yao, J. W. Ciszek, J. M. Tour and R. Shashidhar, *Nat. Mater*., 2006, **5**, 901–908.
100 H. van Zalinge, W. Haiss, R. J. Nichols, J. A. Smerdon and R. McGrath, unpublished data.
101 A. Nitzan and M. A. Ratner, *Science*, 2003, **300**, 1384–1389.
102 Y. Q. Xue, S. Datta and M. A. Ratner, *J. Chem. Phys*., 2001, **115**, 4292–4299.
103 A. R. Rocha, V. M. Garcia-Suarez, S. W. Bailey, C. J. Lambert, J. Ferrer and S. Sanvito, *Nat. Mater*., 2005, **4**, 335–339.
104 S. Y. Quek, L. Venkataraman, H. J. Choi, S. G. Loule, M. S. Hybertsen and J. B. Neaton, *Nano Lett*., 2007, **7**, 3477–3482.
105 J. B. Neaton, M. S. Hybertsen and S. G. Louie, *Phys. Rev. Lett*., 2006, **97**, 216405.
106 M. Koentopp, K. Burke and F. Evers, *Phys. Rev. B: Condens. Matter Mater. Phys*., 2006, **73**, 121403.
107 S. H. Ke, H. U. Baranger and W. T. Yang, *J. Chem. Phys*., 2007, **126**, 201102.
108 S. Y. Quek, M. Kamenetska, M. L. Steigerwald, H. J. Choi, S. G. Louie, M. S. Hybertsen, J. B. Neaton and L. Venkataraman, *Nat. Nanotechnol*., 2009, **4**, 230–234.